ENERGY HARVESTING USING FREQUENCY VIBRATION OF MEMS STRUCTURE

Parichay Das
Programmer Analyst Trainee
Cognizant Technology Solutions India Private Limited
Email: Parichaydas@yahoo.com

Avigyan Datta Gupta
Programmer Analyst Trainee
Cognizant Technology Solutions India Private Limited
Email: avigyan1@gmail.com

Abstract: *Research into energy harvesting from ambient vibration sources has attracted great interest over the last few years, largely as a result of advances in the areas of wireless technology and low-power electronics. One of the mechanisms for converting mechanical vibration into electrical energy is the use of piezoelectric materials, typically operating as a cantilever in a bending mode, which generate a voltage across the electrodes when they are stressed. Typically, the piezoelectric materials are deposited on a non-electro-active substrate and are physically clamped at one end to a rigid base. So far different models of cantilever structures like simple cantilever, tuning fork etc., have been proposed as energy harvesting modules but the problems with them, has been that they offer very high input impedance resulting in very small current drawn into the network followed to the energy harvesting device.*

The work on energy harvesting using MEMS thus far focused on mainly different cantilever structures which faces the problems like high impedance, low current and low energy convergence efficiency. So the motivation behind this project is to minimize the loss during energy conversion, to make high resonant frequency structure so as to minimize electrode spacing to maximize the current output and to make the low power devices self powered without any environmental impact. Thus, in this work, we propose a diaphragm based MEMS structure to increase the mechanical to electrical conversion efficiency through surface acoustic wave propagation (The purpose can somewhat be achieved by placing the electrodes (typically Inter Digited Electrode) according to the wavelength corresponding to the natural frequency of vibration).The design of electrodes like the electrode spacing and dimensions on the piezo-electric layer will be optimized for maximum energy transfer.

Key words –*Free Standing Cantilever Design, Cantilever Design, Piezoelectric*

1. INTRODUCTION

Energy harvesting (also known as power harvesting or energy scavenging) is the process by which energy is derived from external sources (e.g., solar power, thermal energy, wind energy, salinity gradients, and kinetic energy), captured, and stored for small, wireless autonomous devices, like those used in wearable electronics and wireless sensor networks. Research into energy harvesting from ambient vibration sources has attracted great interest over the last few years, largely as a result of advances in the areas of wireless technology and low-power electronics. One of the mechanisms for converting mechanical vibration into electrical energy is the use of piezoelectric materials, typically operating as a cantilever in a bending mode, which generate a voltage across the electrodes when they are stressed. The structures usually consist of a supporting platform, with one end clamped to a rigid base and the other end free to move. Piezoelectric materials are deposited on either one side (unimorph) or both sides (bimorph) of the platform in such a way that the films can be stressed to generate charges as a result of the d31 mode of the piezoelectric effect. So far different models of cantilever structures like simple cantilever, tuning fork etc., have been proposed as energy harvesting modules but the problems with them, has been that they offer very high input impedance resulting in very small current drawn into the network followed to the energy harvesting device. Thus, in this work, we propose a diaphragm based MEMS structure to increase the mechanical to electrical conversion efficiency through surface aoustic wave propagation. The design of electrodes like the electrode spacing and dimensions on the piezo-electric layer will be optimized for maximum energy transfer. One of the earliest examples of thick-film energy harvesters, based on cantilever configuration, is described by Glynne-Joneset al [1]. The harvester was fabricated by screen-printing a layer of PZT (type-5H) with a thickness of 70 μm on both sides of a stainless steel beam of length 23 mm and thickness 100 μm, to form a bimorph cantilever. The device had a resonant frequency of 80.1 Hz and produced up to 3 μW of electrical power when driving into an optimum resistive load of 333kΩ.Another example, which uses stainless steel as the supporting platform, is described by Roundy et al [2]. The structure has a bimorph configuration and consisted of two sheets of PZT attached to both sides of the steel beam, which acts as the centre shim. The structure has an overall size of about 1 cm3, including a proof mass that is attached at the tip of the cantilever. When excited at 100 Hz with an input acceleration of 2.25 m s−2, it produced an output power of about 70 μW when driving into a resistive load of 200 kΩ. Sodano et al [3] have used aluminium plates of thickness 63.5 μm as the supporting platforms and have attached piezoceramic PZT and macro-fiber composite (MFC) samples in order to compare the efficiency of the active materials, and also the time taken, for charging batteries. The PZT sample was PSI-5H4E piezoceramic from Piezo Systems Inc. having a length of 62.5 mm and a width of 60.32 mm, while the MFC sample was a thin PZT fiber film developed by NASA. The fibers were embedded in a Kapton film of dimensions 82.55 × 57.15 mm and having an interdigitated electrode (IDE) pattern, which allows the device to be operated in the d33piezoelectric mode rather than the d31 mode, which has a lower magnitude. From the experiments, they concluded that the PZT piezoceramic performed better than the MFC sample. Despite the higher value of

d33 compared to d31, the electrical current produced by the MFC sample was very small and not suitable for power harvesting. An example of a device that uses silicon as the supporting platform is described by Jeon et al [4]. The cantilever, with dimensions of 170 μm × 260 μm, had a fundamental resonant frequency of 13.9 kHz and was able to generate an electrical power of 1 μW at a base displacement of 14 nm, when driving into a resistive load of 5.2 MΩ. There are many other micromachined silicon cantilevers described in the literature [5–7], although most of these are used in biochemical detection applications rather than energy harvesting.

A free-standing structure is one that stands alone (or on its own foundation) and is free from external support or attachment to a non-electroactive platform. One of the advantages of free-standing thick-film structures is their ability to provide a support structure upon which other sensing materials can be deposited. Such structures are three-dimensional micromechanical structures and are analogous to silicon micro-machined MEMS [8]. The main difference is that free-standing thick-film structures are formed without the need for a supporting platform, which are passive mechanical elements that do not directly contribute to the generation of electrical energy. It is therefore desirable for them to be thin and flexible. Free-standing thick-film devices are multilayered structures comprising only screen-printed piezoelectric materials and electrodes. Their mechanical (e.g. Q-factor and elastic constants) and electrical properties (piezoelectric coefficients and coupling factor) can be measured in the absence of the supporting platform. Free-standing thick-film structures can be fabricated using mass-production methods and do not need to be assembled manually, unlike some other devices described in the literature [1, 2, 3]. It is therefore possible to create quite complex structures with a series of relatively simple fabrication steps. They can also be integrated with other thick-film layers and microelectronic components, thereby offering an interesting alternative to micromachined MEMS. Circular membranes (a form of free-standing structure), or use as a pressure sensor and fabricated with thick-film technology, were first described by Stecher over 20 years ago [9]. Since then, however, there has been very little concerted effort to apply thick-film technology for fabricating free-standing piezoelectric transducers. Bulk piezoelectric materials can be measured with either static or dynamic measurement methods. The measurement of thick-film piezoelectric, however, is not straightforward because the films are attached to a substrate, the effect of which is to introduce a boundary condition on the active material. The longitudinal piezoelectric charge coefficient, d33, cannot therefore be measured directly because of the influence of additional electrical charge produced as a result of the transverse piezoelectric, d31 effect. The properties of thick-film piezoelectric materials are therefore inferred accounting for the measurement errors [10]. Free-standing unimorph structures, with a laminar layer of PZT sandwiched between upper and lower electrodes can serve as a characterization tool, to investigate the mechanical and electrical properties of piezoelectric materials.

2. FREE STANDING CANTILEVER DESIGN

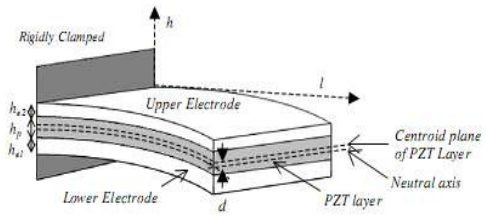

Figure 1 A schematic diagram of a free-standing cantilever structure.

A free-standing unimorph cantilever structure with upper and lower electrodes bonded together with a PZT layer and rigidly clamped at one end is illustrated in figure 1. The cantilever is free to move at the opposite end when operating in a bending mode so that the PZT material is stressed to produce electrical output voltage. The magnitude of the output voltage depends on the distance between the centroid of the PZT layer and the neutral axis of the material d. A bending cantilever is subjected to tensile and compressive stresses that are proportional to the distance above and below the neutral axis, respectively. There is no resultant stress, σ, acting on the neutral axis over the cross-section area, A, and since the elastic modulus, E, and the curvature of the bending cantilever, κ, are not zero, the integral of the distance from the neutral axis over the cross-sectional area can be written as

$$\int_A \sigma \, dA = -\int_A E\kappa h \, dA = \int_A h \, dA = 0. \qquad (1)$$

The composite beam can be analyzed with the transformed-section method [11], where the cross-section of a composite beam is transformed into an equivalent cross-section of an imaginary beam that is composed of only one material with an elastic modular ratio

$$\eta_E = E_e / E_p \qquad (2)$$

Where E_e is the elastic modulus of the electrode layer and Ep is the elastic modulus of the PZT layer. Therefore, the distance from the centroid of the PZT layer to the neutral axis of a composite structure with thickness of PZT, h_p, lower electrode, h_{e1}, and upper electrode, h_{e2}, is

$$d = \frac{1}{2}h_p - \frac{h_p^2 + n_E\left(h_{e1}^2 - h_{e2}^2 + 2h_p h_{e1}\right)}{2\{h_p + n_E(h_{e2} + h_{e1})\}}. \qquad (3)$$

The transverse natural frequency of the composite cantilever with a length, l_b, larger than its thickness, hb, ($l > 50\ h$) can be derived from the Bernoulli– Euler beam equation as [12]

$$f_i = \frac{v_i^2}{2\pi l_b^2}\sqrt{\frac{D}{m_w}} \qquad (4)$$

Where v_i is a coefficient related to boundary conditions (and has a value of 1.875 for the fundamental resonant mode), mw is the mass per unit area of the cantilever and D is the bending modulus per unit width given by [11]

$$D = \sum_{i=1}^{n} E_i \int (h - h_N)\, dh. \qquad (5)$$

To estimate the natural frequency of the composite unimorph cantilever, the thicknesses of the electrodes are assumed to be symmetric; therefore, the neutral axis is coincident with the centroid of the PZT layer and the bending modulus per unit width of the structure is

$$D_{\text{unimorph}} = \tfrac{1}{12}E_p h_p^3 + \tfrac{2}{3}E_e\left(h_e^3 + \tfrac{3}{4}h_p^2 h_e + \tfrac{3}{2}h_p h_e^2\right). \qquad (6)$$

Assuming that the lengths of the piezoelectric and electrodes are similar (i.e. equal to lb) and the thickness of the upper and lower electrodes is he, therefore the mass per unit area of the cantilever for a unimorph is

$$m_w = \rho_p h_p + 2\rho_e h_e. \qquad (7)$$

Substituting equations (6) and (7) into (4) gives the fundamental natural frequency

$$f_N = \frac{0.1615}{l_b^2}\sqrt{\frac{E_p h_p^3 + 8E_e\left(h_e^3 + \frac{3}{4}h_p^2 h_e + \frac{3}{2}h_p h_e^2\right)}{\rho_p h_p + 2\rho_e h_e}}. \quad (8)$$

Ideally, a cantilever structure with a low natural frequency is desirable for a miniature, integrated system. As the size scales down, however, the resonant frequency scales up, and hence an additional proof mass is needed at the end of the cantilever. The natural frequency for a cantilever with proofmass, f_M, can be obtained by comparing the natural frequency of a cantilever without proof mass as

$$f_M = f_N\sqrt{\frac{m_{\text{eff}}}{m_{\text{eff}} + M_m}} \quad (9)$$

Where M_m is the additional proof mass and meff is the effective mass at the tip of the cantilever, which is given by [12]

$$m_{\text{eff}} = 0.236\, m_b \quad (10)$$

Where m_b is the total mass of the composite cantilever structure. The output voltage of a piezoelectric cantilever can be estimated with the model developed by Roundy et al [13]. The complex equation for the output voltage of a piezoelectric cantilever when excited to its resonant frequency ω_r is

$$V = \frac{3}{4}\frac{jE_T d_{31} h_p d}{\varepsilon l_b^2\left\{\zeta_T\omega_r^2 - j\left[\frac{\omega_r^2 k_{31}^2}{2} + \frac{\zeta_T\omega_r}{RC_p}\right]\right\}}a_{\text{in}} \quad (11)$$

Where aim is the base input acceleration, ε is dielectric constant of the piezoelectric material, ζT is the total damping ratio (the sum of electrical and mechanical damping ratio), CP is the capacitance of the piezoelectric material and E_T is the elastic modulus of the composite structure. As the total stress in the composite structure is the sum of the stresses in the PZT layer and the electrode layer multiplied by their relative cross-sectional areas, therefore the total elastic modulus is

$$E_T = (1 - A_p)E_e + A_p E_p \quad (12)$$

Where Ap is the cross-sectional area of the PZT layer. Although the model is somewhat over simplified, it does give a reasonably good approximation for the voltage generated and will be used to compare with the experimental results in this work. The electrical output power is calculated using the expression $P=|V|^2/2R$

3. MEASUREMENT OF THE PIEZOELECTRIC PROPERTIES OF FREE-STANDING THICK FILMS

There is no constraint on the movement and no further influence of external materials on free-standing films; therefore, the properties of the films can be determined by direct measurement similar to that used to measure bulk samples. Both the static and dynamic measurement methods to determine the properties of our PZT samples have been used by the authors.

3.1 STATIC MEASUREMENT

Static measurements are performed by directly applying a variable force to the piezoelectric material and measuring the charge generated. The piezoelectric charge coefficient obtained by this method (Berlincourt method) [14] is given by

$$d_{ij} = \frac{\text{Short circuit charge density in } i \text{ direction}\ [\text{C}]}{\text{Applied stress in } j \text{ direction}\ [\text{N}]}. \quad (13)$$

The subscript i and j is the notation for the poling direction and applied stress direction, respectively. The piezoelectric charge coefficient, d33, can be measured directly with the commercial Berlincourt piezometer system (www.piezotest.com), as shown in figure 2. This can be used to calculate another useful parameter, the longitudinal voltage coefficient, g33, which is related to the permittivity of the material ϵ^T_{33} given by

$$g_{33} = \frac{d_{33}}{\varepsilon_{33}^T}. \quad (14)$$

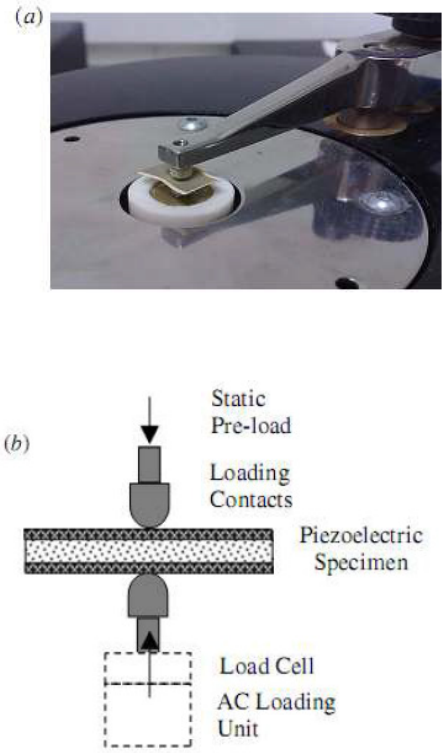

Figure 2 (a) A photograph and (b) A schematic diagram showing a piezoelectric specimen being measured by the Berlincourt measurement method.

The permittivity of the material is related to the capacitance Cp at constant (or zero) applied stress and the dimensions of the material (thickness, h, and area, A) as shown in equation 15. The capacitance measurements are usually carried out at 1 kHz and at low excitation voltages (typically a few millivolts)[15].

$$\varepsilon_{33}^{T} = \frac{C_p h}{A}. \qquad (15)$$

Two samples of PZT with different co-firing profiles were compared. The piezoelectric charge coefficient decayed as continuous varying stress was applied to the materials. This is a common phenomenon for piezoelectric materials and arises because of several factors, including the presence of a defective interface layer, which can give rise to the back switching of domains [16]. As shown in figure 3, PZT samples co-fired at a peak temperature of 950^{0}Chavea d33 value of around 80 pC N−1and samples co-fired at a peak temperature of 850 ◦C [17] have a lower value of only 50 pC N^{-1}after 8 h of measurement. It should be noted, however, that higher temperature processes tend to produce more cracks in the composite structures, particularly at the connecting area between the cantilever beam and the base. The cracks can prevent the free-standing structure from responding to the mechanical excitation accordingly and also cause electrical shorting between the electrodes.

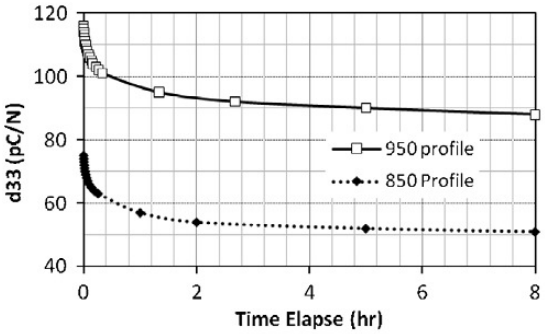

Figure 3 **Piezoelectric charge coefficient d33 decay over 8 h for samples with a cofired profile at peak temperatures of 850 ^{0}C and 950 ^{0}C.**

3.2 DYNAMIC/RESONANT MEASUREMENT

The resonant measurement technique is an example of a dynamic method commonly used to determine the piezoelectric and elastic properties of piezoelectric and was first proposed by Mason and Jaffe in 1954 [18]. The technique involves the measurement of the resonant and antiresonant frequencies, which correspond to the minimum and maximum impedances of a piezoelectric material. Since these frequencies can be accurately measured, this method provides a good basis for determining the properties of bulk (or freestanding) piezoelectric materials. As the thickness of the samples was many times smaller than their widths and lengths (h <w/50 and h < l/100), this method is suitable for measuring the piezoelectric constants related to transverse modes, where the direction of polarization is perpendicular to the direction of the applied stress. The transverse piezoelectric charge coefficient is given as [18].

$$d_{31} = \frac{1}{2\pi f_r}\sqrt{\frac{\varepsilon_{33}^{T}}{\rho\left\{1+\frac{8}{\pi^2}\left(\frac{f_r}{2\Delta f}\right)\right\}}}. \qquad (16)$$

This is related to the resonant frequency, fr, the difference between resonant and antiresonant frequencies, Vf ,the density, ρ, and the permittivity of the piezoelectric materials. The effectiveness of energy conversion between electrical and mechanical is indicated by the coupling factor, which can be determined using

$$k_{31} = \frac{d_{31}}{\sqrt{\varepsilon_{33}^{T} s_{11}^{E}}} \qquad (17)$$

Where S_{11}^{E} is the elastic compliance at a constant electric field of the material, which can be calculated from

$$s_{11}^{E} = \frac{1}{\rho\,(2l_b f_r)^2}. \qquad (18)$$

4. CHARACTERIZATION OF THICK FILM,FREE STANDING STRUCTURES

The mechanical Q-factor is an important parameter that quantifies the energy dissipation through vibration. Generally, the losses can be categorized as either external or internal [19]. The external losses are due to airflow and radiation of elastic waves at the area where the cantilever was being clamped, while the internal losses are caused by surface loss and thermo elastic loss [20]. We were interested to investigate the effect of the length of the beam on the Qfactor of the cantilever structure. This can be used to calculate the efficiency of the structure in converting mechanical energy to electrical energy. The total Q-factor, Q_T , of the structure can be determined experimentally by exciting the free-standing structures on a shaker table, over a range of frequencies around their resonant frequency. The output was measured on a network analyzer. The shaker table was operated in a sinusoidal vibrational manner, driven by an alternating current source from an amplifier over a range of frequencies from a function generator. The acceleration of the shaker was kept at a constant level using a feedback system, where the accelerometer in the shaker has a resonant frequency of around 230 Hz, while shorter cantilevers, with a length of 4.5mm, have a resonant frequency of about 2300 Hz. Attaching additional proof masses to the cantilever beam can further reduce the resonant frequency. The measurement results also showed that the natural frequency of the structure is not affected by the distribution of the proof masses. A shorter or longer cantilever does not appear to exhibit the same Qfactors as those having a square structure. This is because shorter or longer cantilever structures suffer losses at different rates and with different dominant factors. The energy dissipation loss at the support is dominant for a shorter structure [21], while air-damping losses become dominant for longer cantilever structures [22].

4.1 EVALUATION OF ELECTRICAL OUTPUT

A modest electrical power output (a few nano-watts) was produced when the composite unimorph structure was operated in its bending mode. The output power is affected by the distance from the centroid of the piezoelectric material layer to the neutral axis of the composite cantilever, d. The electrical output power from the devices was measured by connecting the lower and up electrodes to a programmable load resistance and then converting the voltage into a digital signal to be measured with a National Instruments Sequence Test programmed. A series of different experiments was carried out to investigate the output power as a function of cantilever length, electrical load resistance, proof mass and input acceleration level. By careful selection of resistive loads, the electrically induced damping can be adjusted so that it is equal to mechanical damping. Once the optimal resistive load is obtained, the maximum output power is produced.

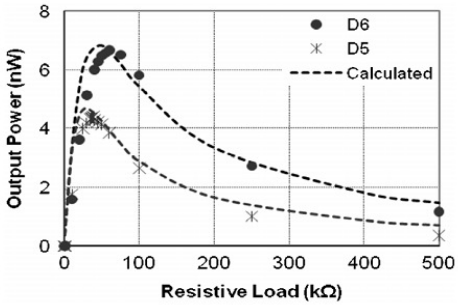

Figure 4 Output power at resonant frequency as a function of electrical resistive load when accelerated at a level of 100 milli'g'(≈1ms−2).

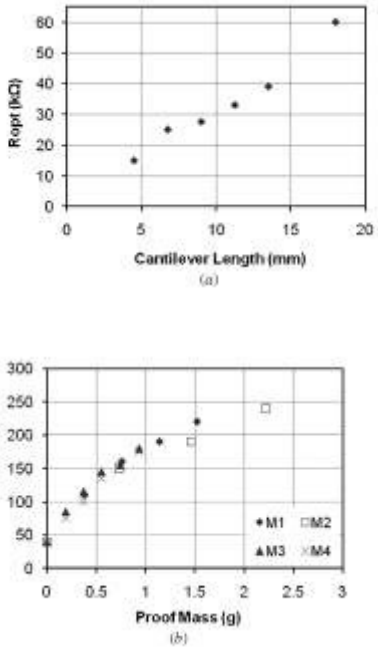

Figure 5 Optimum resistive load, Ropt , as a function of (a) cantilever length and (b) proof mass

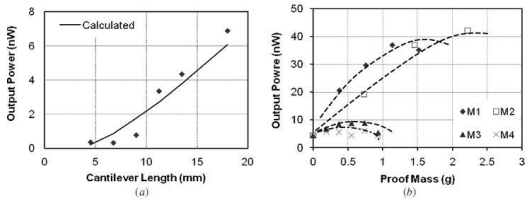

Figure 6 Output power at optimum resistive load as a function of (a) cantilever length and (b) proofmass for sample loaded with different distributions of proof masses. (The dotted line Is a guide to show the pattern of the change)

Figure 4 shows the experimental and calculated results for samples when excited to their resonant frequencies at an acceleration level of 100 milli 'g' (≈1ms−2). The optimum output power is obtained by driving into resistive loads of 60 kΩ and 39 kΩ, respectively. The required value for the resistive load was found to be a function of the length of the cantilever, as shown in figure 5(a). It is further increased when proof masses are attached, as shown in figure 5(b). The optimum resistive load for sample D5 saturates at around 250 kΩ, with an added proof mass exceeding 1.5 g. The distribution of the masses does not seem to influence the value of the optimum resistive load. The distribution of the proof masses, however, has a significant influence on the output power, as shown in figure 6(b). Sample D5 with attached proof masses of dimensions M1 produces a maximum output power of about 40 nW, which is more than a factor of 8 higher than a device without the proof mass. M1 has a distribution of masses focused at the tip of the cantilever and appears to have imposed the maximum allowable stress on the cantilever, before a reduction of power due to energy losses from mechanical damping at greater values of added mass (>1.2 g). Proof masses having broader distribution areas on cantilever M2 can increase beyond this before mechanical damping becomes dominant. The larger mass of M2, however, does not show a significant improvement in the output power, and furthermore, it is not desirable to stress the fragile ceramic cantilever beyond 8.5MPa (experimental maximum stress point found in[1]). In this case, an acceleration level of 1ms−2 allows a maximum mass of around 2.8g. M3 and M4, respectively, have a mass distribution towards the centre spine of the cantilever and show inferior output power levels of less than a quarter the value of the maximum power stored in the piezoelectric materials.

4.2 ELECTRICAL OUTPUT IMPROVEMENT

Mulitmorph structures were fabricated using a co-firing profile of 950^0C. They comprise three laminar sections of PZT having equal thicknesses of about 40μm and physically separated by thin layers of Ag/Pd electrodes of equal thickness (12 μm) as shown in figure 7. Using the same fabrication method as used for the unimorph structures, the upper and lower electrodes of the composite ultimorph cantilevers were also covered with a thin layer of PZT, with a thickness of 10 μm. Since the lower and upper layers of piezoceramic are displaced further from the neutral axis, a significant improvement in the electrical output (as predicted from equation (11)) is expected.

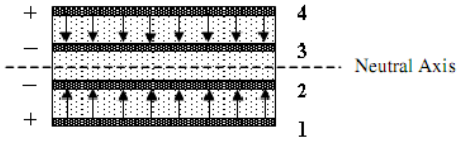

Figure 7 Cross-sectional view of a mulitmorph structure. The number beside each layer denotes the fabrication sequence of electrode plates. A mulitmorph sample having a total thickness of 168 μm and a length of 18 mm was used to investigate the electrical output performance. The mulitmorph structure was polarized at 220 V in series by connecting the outer electrodes to the positive terminal and the inner electrodes to the negative terminal of the dc power source, at a temperature of 200 C for 30 min. The outer electrode plates were polarized in the same direction towards the centre plates, and this produced a neutral polarity at the centre piezoelectric layer, which is also served as a mechanical neutral axis to the structure. This central layer is not similar to the traditional supporting platform because it is electro-active and therefore has the potential to product an electrical output when a correct configuration of electrode terminals is in place.

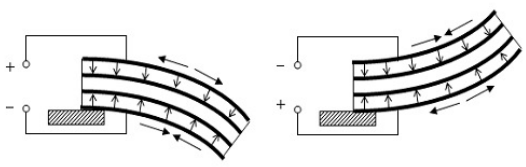

Figure 8 A diagrams showing downward and upward bending positions of a mulitmorph cantilever, which produces an alternating output voltage at the output terminal.

When the cantilever resonates, as shown in figure 8, an alternating voltage is produced. At a point where the cantilever bends downwards, tensile forces on the upper piezoelectric element (perpendicular to the direction of polarization) generate voltages of the same polarity as the poling voltage. The compressive forces on the lower piezoelectric element generate a voltage of opposite polarity to that of the poling voltage and vice versa, when the cantilever is bent upwards. The open circuit voltages across a few combinations of electrodes were investigated. Ideally, the open circuit voltages across terminals 3 and 4 (upper section of PZT) and terminals 1 and 2 (lower section of PZT) are similar, but experimentally there is a discrepancy in the output voltage between the upper and lower sections of PZT. This is because the neutral axis is not precisely coincident with the centroid of the PZT layers. PZT sections with larger d (distance from the neutral axis to the centroid of the PZT layer) produce greater output voltages.
The open-circuit voltage across terminals 1 and 4, with a short between the two centre electrodes 2 and 3, is equivalent to a series connection of two piezoelectric impedance components and produces a total voltage that is equal to the sum of the individual lower and upper sections of the PZT. An open circuit voltage exceeding 2.5 V was measured at a resonant frequency of 400 Hz when driven at an acceleration level of 1.5 ‘g’(≈15ms−2), as shown in figure 9. An equivalent circuit of parallel connection is produced when a positive terminal (made by connecting electrodes 1 and 4), and negative terminal (made by connecting the central electrodes 2 and 3) are measured. Maximum output power can be obtained by loading the mulitmorph structure with a range of resistances at its resonance frequency as shown in figure 10. The upper and lower sections of the PZT produce a maximum output power of 25 µW and 33 µW, respectively, when driving similar resistive load at 18.5 kΩ, at an acceleration level of 0.5 g. The output power is scaled up when connecting the individual lower and upper sections to make a series configuration and this produced a maximum power of about 40 µW, when driving a greater resistive load of 37.5 kΩ. The magnitude of the output power is significantly improved by a factor of about 400 compared to a unimorph composite structure of similar length.

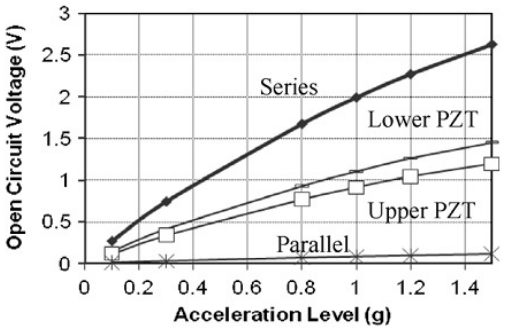

Figure 9 Open circuit voltage as a function of the acceleration level for a mulitmorph cantilever with different electrode configuration.

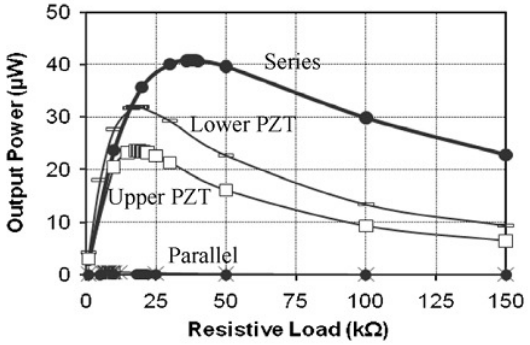

Figure 10 Output power as a function of resistive load for a mulitmorph cantilever with a few different electrode configurations.

5. WORK DONE

5.1 MEMS STRUCTURE

The structure proposed in this paper is a circular membrane with a proof mass at the centre. The design is expected to generate vibration at the centre and the energy will propagate through the membrane generating surface acoustic wave.

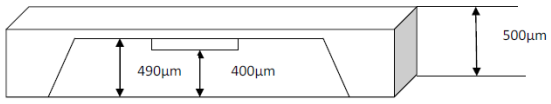

Figure 11 ***Simple cross-sectional view of the proposed MEMS structure***

5.2 FABRICATION

To fabricate the membrane structure using COVENTERWARE the steps are

- The substrate chosen as Silicon [100] with a square base of 10mm×10mm and height is fixed at 490µm.
- Next a wet anisotropic etching is performed with a positive circular photo mask at centre with radius 1mm.
- Now finally another anisotropic wet etching is performed with a negative photo mask at the centre and radius of 3mm.

. Now are left with a circular membrane of 10µm thickness and radius 3mm, and the proofmass of 100µm thickness and 2mm diameter.

Figure 12 ***Bottom view of the MEMS structure after fabrication***

5.3 SIMULATION

The MEMS structure then analyzed using COVENTERWARE for finding the modal frequencies. Modal analysis is performed in the

meshed model of the MEMS design. Modal analysis is applied up to 4 different modes and the following results are obtained.

(i) Mode1 (fundamental mode):

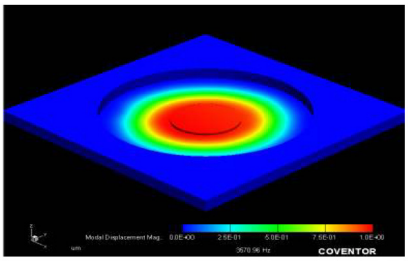

Modal frequency 3.5KHz

(ii) Mode 2

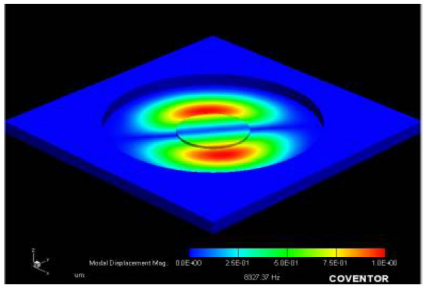

Modal frequency 8.2KHz

(iii) Mode 3

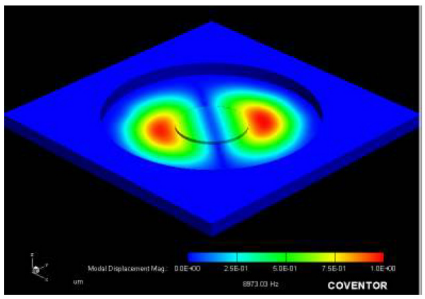

Modal frequency 8.97KHz

(iv) Mode 4

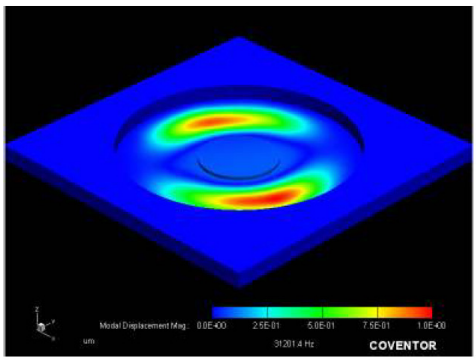

Modal frequency 31.2KHz

6. CONCLUSION

The modal analysis performed on the proposed MEMS design shows that the fundamental frequency of vibration is around 3 KHz which is not sufficient enough for generating surface acoustic wave on the membrane developed. Thus modification on the design should be carried out on the model dimensions or shape. Also the modal harmonic analysis should be carried out to find the responses with varying frequency. Once the modal frequency is known we can find out electrode spacing for ensuring maximum conversion of mechanical energy to electrical energy. Electrode shape will also be a design concern

7. REFERENCES

1) Glynne-Jones P, Beeby S P and White N M 2001 Towards a piezoelectric vibrationpowered microgenerator IEE Proc. Sci. Meas. Technol 148 68–72.

2) Roundy S, Wright P K and Rabaey J 2003 A study of low level vibrations as a power sources for wireless sensor nodes Comput. Commun. 26 1131–44.

3)Sodano H A, Inman D J and Park G 2005 Comparison of piezoelectric energy harvesting devices for recharging batteries J. Mater. Sci., Mater. Electron. 16 799–807.

4) Jeon Y B, Sood R, Jeong J and Kim S-G 2005 MEMS power generator with transverse mode thin film PZT Sensors Actuators A 122 16–22.

5) Itoh T and Suga T 1996 Self-excited force-sensing microcantilevers with piezoelectric thin films for dynamic scanning force microscopy Sensors Actuators A 54 477–81.

6) Yi J W, Shih W Y and Shih W H 2002 Effect of length, width, and mode on the mass detection sensitivity of piezoelectric unimorph cantilevers J. Appl. Phys. 91 1680–6.

7) Lu J, Ikehara T, Zhang Y, Mihara T, Itoh T and Maeda R 2008 High quality factor silicon cantilever driven by PZT actuator for resonant based mass detection Proc. Design,Test, Integration & Packaging of MEMS/MOEMS (DTIP) (Nice, France, 9–11 April 2008).

8) White N M and Turner J D 1997 Thick-film sensors: past, present and futureMeas. Sci. Technol. 8 1–20.

9) Stecher G 1987 Free supporting structures in thick-film technology: a substrate integrated pressure sensor Proc. 6th European Microelectronics Conf., Bournemouth pp 421–7.

10) Torah R N, Beeby S P and White N M 2004 Experimental investigation into the effect
of substrate clamping on the piezoelectric behaviour of thick-film PZT elements J. Phys. D: Appl. Phys. 37 1074–8.

11) Gere J M 2001 Mechanics of Materials 5th edn (Pacific Grove, CA: Brooks/Cole).

12) Merhaut J 1981 Theory of Electroacoustics (New York: McGraw-Hill).

13) Roundy S and Wright P K 2004 A piezoelectric vibration based generator for wireless electronics Smart Mater. Struct. 12 1131–42.

14) Jordan T, Ounaies Z, Tripp J and Tcheng P 1999 Electrical properties and power considerations of a piezoelectric actuator Proc. Material Research Society Symp.(December 1999) pp 203-8.

15) Shepard J F Jr, Chu F, Kanno I and Trolier-McKinstry S 1999 Characterization and aging response of the d31 piezoelectric coefficient of lead zirconate titanate thin films J.Appl. Phys.85 6711–6.

16) Torah R N, Beeby S P and White N M 2004 Improving the piezoelectric properties of thick-film PZT: the influence of paste composition, powder milling process and electrode material Sensors Actuators A 110 378–84.

17) Mason W P and Jaffe H 1954 Methods for measuring piezoelectric, elastic, and dielectric coefficients of crystals and ceramics Proc. IRE 42 921–30.

18) Jinling Y, Ono T and Esashi M 2002 Energy dissipation in submicrometer thick singlecrystal silicon cantilevers J. Microelectromech. Syst. 11 775–83.

19) Yasumura K Y et al 2000 Quality factors in micron- and submicron-thick cantilevers J.Microelectromech. Syst. 9 117–25.
20) Sandberg R, Lhave K, Boisen A and Svendsen W 2005 Effect of gold coating on the Qfactor of a resonant cantilever J. Micromech. Microeng. 15 2249–53.
21) Nouira H, Foltete E, Hirsinger L and Ballandras S 2007 Investigation of the effects of air on the dynamic behaviour of a small cantilever beam J. Sound Vib. 05 243–60.
22) Energy harvesting MEMS device based on thin film piezoelectric cantilevers by W.J.Choi · Y. Jeon · J.-H. Jeong · R. Sood · S.G. Kim.

Parichay Das was born in Midnapore, West Bengal, India, on 5th March, 1989. He received the B. Tech degree in Electrical Engineering from College of Engineering & Management, Kolaghat (WBUT University), India, 2011.He is currently Programmer Analyst Trainee at Cognizant Technology Solutions India Private Limited. From the beginning of his B. Tech career, he is involved in several projects & Workshops. He successfully completed 6 numbers of projects in his academic career and some project work done from Jadavpur University, IT Kharagpur and Bengal Engineering and Science. He has already published 2 research papers in National Conference proceedings & one International Journal Paper. His area of interest in Power System, Electrical Machine, Control System Visual Cryptography, Analog/Mixed Signal VLSI and MEMS and renewable energy field

Avigyan Datta Gupta was born in Kolkata, West Bengal, India, on 16th August, 1986. He received the B. Tech degree in Electronics & Instrumentation Engineering from Future Institute of Engineering & Management, Sonarpur (WBUT University), India, 2011.He is currently Programmer Analyst Trainee at Cognizant Technology Solutions India Private Limited. From the beginning of his B. Tech career, he is involved in several projects & Workshops. He successfully completed 3 numbers of projects in his academic career from Jadavpur University, IIT Kharagpur and Bengal Engineering and Science University, Shibpur. His area of interest in Analog/Mixed Signal VLSI and MEMS.